Energy and Buildings 111 (2016) 290–298

Contents lists available at ScienceDirect

Energy and Buildings

journal homepage: www.elsevier.com/locate/enbuild

# Practical implementation and evaluation of model predictive control for an office building in Brussels

Roel De Coninck[a,b,c,*], Lieve Helsen[a,c]

[a] KU Leuven, Department of Mechanical Engineering, Celestijnenlaan 300, Postbox 2421, 3001 Heverlee, Belgium
[b] 3E nv, Kalkkaai 6, 1000 Brussels, Belgium
[c] EnergyVille, 3600 Waterschei, Belgium

ARTICLE INFO

*Article history:*
Received 27 March 2015
Received in revised form 9 October 2015
Accepted 5 November 2015
Available online 23 November 2015

*Keywords:*
Model predictive control (MPC)
Grey-box models
Field test
Validation
Modelica

ABSTRACT

A model predictive control (MPC) has been implemented in a medium-sized office building in Brussels, Belgium. This paper presents the implementation of the controller and the measured performance in comparison with the default, rule-based control (RBC). The building has two floors and a total size of 960 $m^2$. The controllable system is the hybrid heat production consisting of two air/water heat pumps and a condensing gas boiler. The practical situation does not allow controlling end-units in the different zones of the building. The MPC makes use of a Modelica grey-box control model resulting from a system identification with monitoring data. The paper covers the monitoring, model identification, forecasting of disturbances, state estimation, formulation and solving of the optimal control problem (OCP) and transmission of the control signals. The performance is evaluated on a daily basis based on analysis of heating degree days, thermal comfort, energy costs and primary energy consumption. The results show that the model predictive controller is able to provide a similar or better thermal comfort than the reference control while reducing the energy costs by more than 30%. This is due among others, to a better use of the heat pumps and an adapted hot water supply temperature.



## 1. Introduction

Bad control of energy systems in buildings is responsible for large energy efficiency losses. Even in new and modern buildings, inefficient control and operation often increases the primary energy consumption for heating, cooling and air-conditioning (HVAC) by 20 % or more [1,2].

Model predictive control (MPC) is one of several solutions to improve building control efficiency [3–10]. By specifying high-level objectives and using the power of numerical optimisation, a model predictive controller can automatically adapt to new operating conditions and take into account expected future building dynamics. The controller can also incorporate the delivery of additional services like reserves [11] or peak load reduction [12].

The core of the MPC concept is the optimal control problem (OCP). This mathematical problem is formulated in continuous time as

$$\underset{u}{\text{minimize}} \quad J \tag{1a}$$

$$\text{subject to} \quad F(t, \dot{x}, x, w, y, u) = 0, \tag{1b}$$

$$g(t, \dot{x}, x, y, u) = 0, \tag{1c}$$

$$h(t, \dot{x}, x, y, u) \geq 0, \tag{1d}$$

$$x(0) = x_0. \tag{1e}$$

In this formulation, $t \in [0, t_h]$ is time with $t_h$ the prediction horizon, $u \in \mathbb{R}^n$ is the control signal, $J$ the objective, $F(\cdot)$ is the system model with states $x$, algebraic variables $y$ and disturbances $w$. $g(\cdot)$ and $h(\cdot)$ are additional equality and inequality constraints. $x$, $\dot{x}$, $w$, $y$ and $u$ are all time-dependent but for readability we have omitted the time dependency notation.

MPC is based on the solution of an OCP at every control time step. The OCP is initialised from an estimated state of the system based on measurements (= feedback) and takes into account forecasted disturbances and dynamic system behaviour (= feedforward) [13].

Fig. 1 shows a general overview of the MPC framework that will be detailed and implemented in Section 3.

* Corresponding author at: 3E nv, Kalkkaai 6, 1000 Brussels, Belgium.
*E-mail address:* roel.deconinck@3e.eu (R. De Coninck).

http://dx.doi.org/10.1016/j.enbuild.2015.11.014
0378-7788/

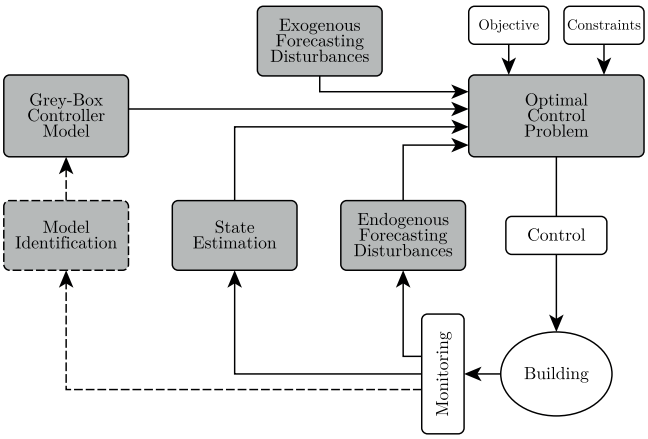


**Fig. 1.** Overview of the MPC framework.

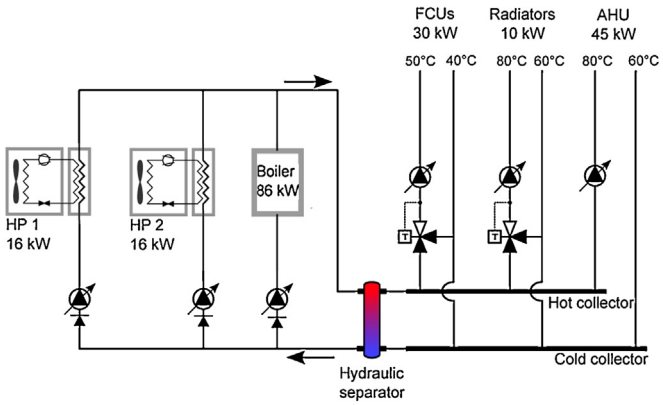


**Fig. 3.** Hydraulic scheme of the heating system.

This paper describes the implementation of MPC in the Kalkkaai building, the headquarters of 3E in Brussels. The implementation with real operating conditions including measurement errors, limitations of the installed control system, communication issues, etc. is an important step in the validation of MPC as viable alternative for controlling real-life buildings. The MPC performance is compared to the conventional control algorithm during the winter of 2014–2015.

This paper is structured as follows. Section 2 gives a general overview of the field test, building and HVAC system and the controllable loads. Section 3 describes the implementation of the MPC by elaborating each step of the tool chain of Fig. 1. The results are presented in Section 4. We compare operational costs, energy use and thermal comfort of the MPC with the conventional control. These results are discussed in more detail in Section 5 where we try to quantify the benefits of the new control strategy for the Kalkkaai building. Finally, Section 6 summarises the conclusions.

## 2. Field test Kalkkaai building

### 2.1. Building

The Kalkkaai building is the headquarter of 3E, situated in Brussels, Belgium. It is composed of two floors of about 480 $m^2$ each and hosts 40–70 people. The building's HVAC and internal zoning has been refurbished in 2013.

Fig. 2 shows the west façade of the building. Despite the large windows, the solar gains are limited in the winter due to the west orientation and the shading of neighbouring buildings. The other façades have much less windows and are even more shaded by other buildings.

**Fig. 2.** View of the Kalkkaai building, west façade.

An overview of the heat production, distribution and emission systems is given in Fig. 3.

The heat production is covered by a condensing gas boiler (nominal power of 86 kW) and two identical air/water heat pumps of 16 $kW_{th}$ each. These three production units are operated in a cascade system.

The heat distribution consists of 3 circuits:

1 fan coil units (FCU) in all office spaces,
2 radiators (in toilets and entrance),
3 air handling unit (AHU).

The building is occupied on weekdays during typical office hours, but large occupancy variation is not unusual. The occupants have manual control over the lighting and temperature setting in each of the rooms.

### 2.2. Control system

The existing reference control is called the *rule-based control* (RBC). Due to the manual control of the FCUs by the occupants, the building energy control and management system (BECMS) cannot control the heat consumption of the building directly. The BECMS controls the hot water supply temperature $T_{Sup}$ to influence the heat consumption indirectly. $T_{Sup}$ is controlled according to a heating curve based on the ambient temperature, with indoor temperature compensation. A proportional-integral (PI) controller tracks this heating curve by controlling the total thermal power to be produced. An example of the resulting hot water supply temperature is given in Section 5, Fig. 11.

A specific cascade controller distributes this power set point over the three heat production units based on a comprehensive set of rules. These rules are composed as a set of *suppression weights* for each heat production unit. The suppression weights are summed for each heat producing unit and sorted from low to high to determine the order in which the three units are started in order to meet the total heat demand. There are many different suppression weights. There is a weight for being off (giving higher priority to units that are already in operation), a weight in case of a disturbance on the unit, a weight based on the units temperature (giving priority to units with a higher temperature). There is also a weight based on the minimum modulation degree of the unit, ensuring that small units get started first. This weight is important because it gives priority to the heat pumps when the total heat demand is low. There are specific weights to avoid the operation of the heat pumps at a low efficiency. When the requested supply water temperature

$T_{Sup} \geq 45\,^{\circ}C$, an additional weight is activated on both heat pumps. Similarly, another weight is added when $T_{Amb} \leq 3\,^{\circ}C$. Both weights ensure that the gas boiler has priority under these circumstances. One particular issue with the cascade control is caused by the slow start-up of the heat pumps. By consequence, during start-up, the asked thermal power will not be produced. Even when the heat pumps have a lower suppression weight, the gas boiler will be activated soon after the heat pumps are started to reduce the difference between the asked and delivered thermal power.

Unfortunately, there is no high-level control of the AHU. The AHU is switched on/off according to a weekly schedule. The same schedule is applied to the hot water circulation pump to the heating coil. There is no feedback on the supply air temperature.

The implementation of MPC as high level control makes use of the BECMS for the low level control. By consequence, the limited options to control the heat supply and supply air temperature affects the MPC as much as the conventional control. The supplier of the BECMS allows to get and set any monitored or controlled variable directly by a file transfer protocol (FTP). The MPC uses this protocol to control the thermal power of the boiler and both heat pumps directly. How these control signals are computed is explained in the next section.

## 3. Implementation of the MPC tool chain

This section elaborates on the practical implementation of the model predictive controller. The different processes of Fig. 1 are discussed in detail.

### 3.1. Monitoring

A Kairos time series database has been set up as central storage for all monitoring data, predictions and control set points. There are different sources for these data.

The BECMS monitors the heat production and distribution at the level of the technical room. There are measurements of several water temperatures, heat fluxes, natural gas consumption and different HVAC related electricity consumptions. The latter include sub-metering for each of the heat pumps and circulation pumps. All relevant monitoring data is extracted from the BECMS using the FTP every 15 s and stored in the Kairos database.

An independent system (from a different manufacturer) monitors the building. We refer to this as the building monitoring system (BMS). The BMS monitors room temperatures, relative humidities and electricity consumptions at building level. The latter include sub-metering for lighting (by floor), plug load (by floor), the server room, the chiller and AHU. The measured data is obtained by posting http requests on a webserver and parsing the returned json objects to upload the data to the Kairos database.

Weather data is obtained from a third source. Through collaboration in the EU FP7 project *PerformancePlus*, the University of Oldenburg, Germany provides both past weather data and weather forecasts [14–16]. These contain ambient temperature, solar radiation, wind speed and relative humidity. This data is posted on a specific FTP-server and processed to time-series that are stored in the Kairos database.

With all these different data sources and systems, the overall monitoring system is vulnerable for failures. Some failures are harmless and only generate extra manual work to recover data and store it in the database, others lead to unrecoverable data loss. Despite the use of different systems, some important variables are not monitored at all, like occupancy, $CO_2$ concentrations, the supply air temperature and the heat consumption of the individual rooms in the building. Also, the room air temperatures are measured at irregular intervals and obtained with delays of up to half an hour. These shortcomings will affect the options for modelling and control as we will see in the next paragraphs. Nevertheless, this represents the real world and it is important to analyse the MPC performance in real conditions.

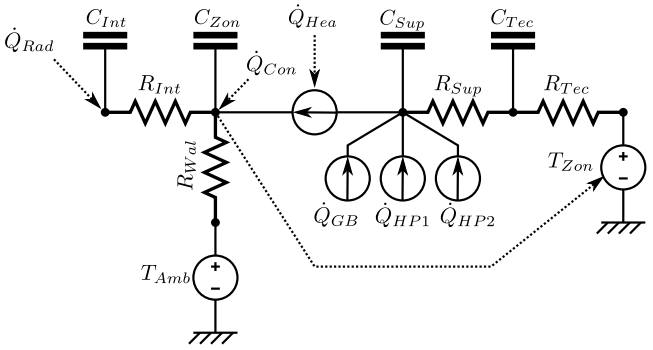


**Fig. 4.** Schematic presentation of the control model for MPC.

### 3.2. Grey-box model identification

The MPC is based on a grey-box control model which has been identified with the *Grey-Box Buildings* toolbox of De Coninck et al. [17]. It is impossible to create a multi-zone building model with the available monitoring data because the heat consumption is only measured at building level. To obtain a single-zone model, all room temperature measurements are arithmetically averaged into $T_{Zon}$. A weighted averaging based on room size would physically be more meaningful, but the required meta-information will often not be readily available for many buildings. In order to demonstrate an MPC that is easily applicable to a wide variety of buildings, we try to limit the use of meta-information as much as possible.

A forward selection method is applied that starts from a first order model and gradually increases complexity until no further improvements in simulation performance can be obtained on the cross-validation dataset [17]. A schematic presentation of the resulting model is given in Fig. 4.

The model has four states: two in the building ($C_{Zon}$ for zone air and $C_{Int}$ for internal mass) and two in the heating system ($C_{Sup}$ for supply water and $C_{Tec}$ for the technical room). The radiative part of internal gains is represented by $\dot{Q}_{Rad}$ and the convective gains/losses of internal gains and the AHU are represented by $\dot{Q}_{Con}$. The heat demand of the building is $\dot{Q}_{Hea}$ and the produced heat of the boiler and both heat pumps is $\dot{Q}_{GB}$, $\dot{Q}_{HP1}$ and $\dot{Q}_{HP2}$ respectively. There are four thermal resistances, $R_{Int}$, $R_{Wal}$, $R_{Sup}$ and $R_{Tec}$. $T_{Amb}$ is the ambient temperature, obtained from a local measurement.

The model does not take into account solar gains. The reason is that during the system identification process, the solar radiation input was not retained as a significant disturbance. This result is explained by the relatively low glazing fraction (except for the west façade), the shading due to neighbouring buildings, and the use of an identification data set with monitoring data of December 2014 and January 2015. The control model is therefore only valid for the winter season, but this is sufficient for this case study. Future research will consider the adaptation of the control model over different seasons.

Internal gains are generated by the use of electrical appliances and body heat gains. For the use of electrical appliances we chose a top-down approach. Starting from the total electricity consumption of the building, we subtract all sub-meters we consider not to correspond to internal gains. For the Kalkkaai building these are the sub-meters for the HVAC system and the servers. A bottom-up approach would only take into account the sub-meters we think correlated with internal gains. By consequence, a top-down

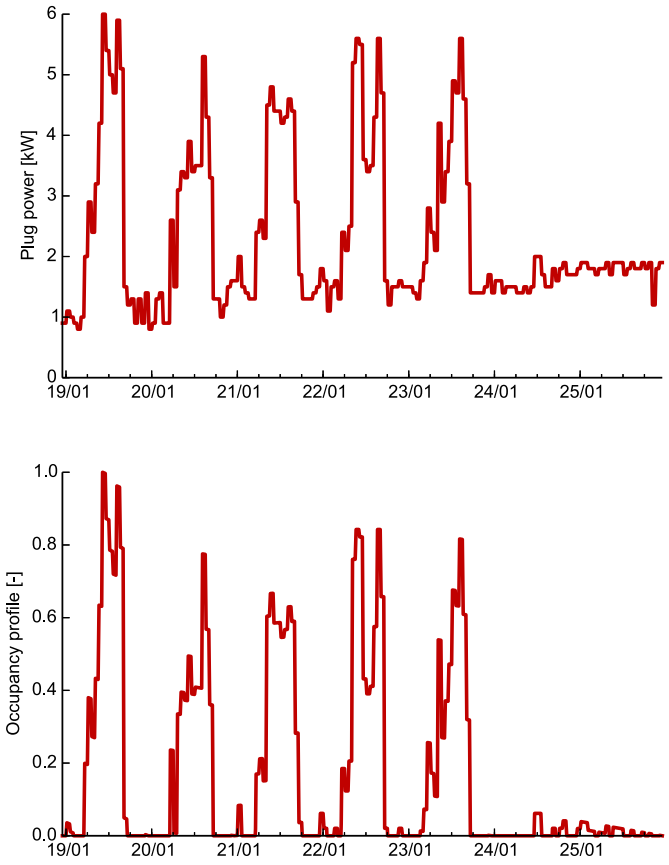


**Fig. 5.** Plug power (top) and derived occupancy profile (bottom) for a typical week.

approach is a maximum estimator of internal gains from equipment and a bottom-up approach a minimum estimator.

There are no direct measurements of internal gains generated by body heat transfer nor of occupancy. However, as plug power is correlated to occupancy, we derive an occupancy profile from the plug power measurement. The standby power consumption is removed by supposing an occupancy of zero persons every night at 00h00 and then the profile is normalised. This is illustrated in Fig. 5. The resulting occupancy profile (between 0 and 1) is used as a disturbance and an additional parameter to be estimated $n_{occ}$ is introduced in the model to represent the number of occupants corresponding to a profile value of one. More details about the forecasting of these disturbances are given in Section 3.3.

The RC scheme in Fig. 4 only represents the dynamic heat transfer processes. The gas consumption $\dot{P}_g$ of the condensing boiler and electricity consumption of both heat pumps $\dot{P}_{HP1}$ and $\dot{P}_{HP2}$ are computed from equations for the boiler efficiency $\eta$ and the coefficient of performance (COP) of the heat pumps, $COP_{HP1}$ and $COP_{HP2}$. These efficiency models are obtained by linear regression on the monitoring data based on the following predictors: $T_{Sup}$, $T_{Amb}$ and the produced thermal power $\dot{Q}_{GB}$ for the boiler or the electrical power $\dot{P}_{HP}$ for the heat pumps [18]. A forward selection is applied to avoid overfitted models. The resulting performance curves are given in Eq. (2).

$$\eta = 0.87 - 8.85e^{-7}\dot{Q}^*_{GB} + 4.82e^{-3}T^*_{Amb} \tag{2a}$$

$$COP_{HP1} = 2.61 + 5.45e^{-2}T^*_{Amb} - 1.23e^{-2}T^*_{Sup} - 1.18e^{-4}\dot{P}^*_{HP1} - 1.54e^{-5}T^*_{Amb}\dot{P}^*_{HP1} \tag{2b}$$

**Table 1**
Overview of endogenous and exogenous disturbances.

| Endogenous | Exogenous |
|---|---|
| Plug power | Ambient temperature |
| Occupancy | Global horizontal radiation[a] |
| Schedule AHU | |

[a] Global horizontal radiation was not retained as significant disturbance in the model identification process.

$$COP_{HP2} = 2.58 + 3.84e^{-2}T^*_{Amb} - 2.50e^{-2}T^*_{Sup} - 1.42e^{-4}\dot{P}^*_{HP2} - 1.50e^{-5}T^*_{Amb}\dot{P}^*_{HP2} \tag{2c}$$

In these equations, the predictor variables are relative values in order to obtain physically meaningful results for the intercept:

$$\dot{Q}^*_{GB} = \dot{Q}_{GB} - 86,000$$

$$\dot{P}^*_{HP} = \dot{P}_{HP} - 6500$$

$$T^*_{Amb} = T_{Amb} - (7 + 273.15)$$

$$T^*_{Sup} = T_{Sup} - (35 + 273.15)$$

It is noteworthy that both heat pumps, though identical, have a slightly different performance model. The OCP will exploit these differences.

### 3.3. Forecasting of disturbances

In the model identification process we have defined different disturbances and estimated the corresponding parameters. We distinguish between endogenous and exogenous disturbances. Endogenous disturbances are measured locally and forecasted based on algorithms we have developed ourselves. Exogenous disturbances can be measured locally or remotely and their forecasts are obtained from external services, typically weather services. A mixture of both is possible, e.g. when an exogenous forecast is corrected based on a local measurement. An overview of both types of disturbances is given in Table 1.

We have implemented the most simple persistence models for the forecasting of all three endogenous disturbances. The forecasted value for $t = t_f$ is the value measured exactly one week before, at $t = t_f - 604{,}800$ s. This is illustrated for plug power in Fig. 6. On some days, like Tuesday 20/01 and in the weekend, we observe a bias, but in general the forecast captures well the general trends of the plug power profile.

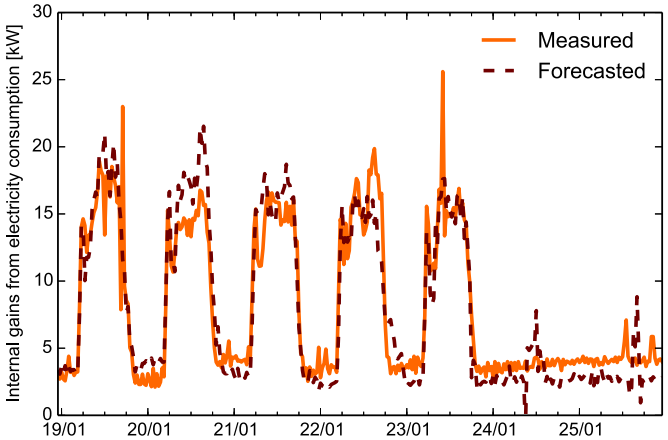


**Fig. 6.** Overview measured and forecasted values for plug power for one week in January 2015.

The forecasts of the exogenous disturbances are provided by a weather service. We obtain these forecasts from the University of Oldenburg in the framework of the EU FP7 project *PerformancePlus*. The only exogenous input in the used model is $T_{Amb}$, the ambient temperature. This temperature is also measured on-site. Differences between the forecasted and measured values of up to 5 K have been observed. In order to take into account local conditions, the forecast is adjusted by the difference between the forecasted value and the measured value for $t = 0$.

### 3.4. State estimation

Since not all states of the control model can be measured, state estimation is a required step in any model predictive control scheme. The state estimation problem boils down to examining the past monitoring data and reconciling these measurements with the model to determine the most likely value of the state at the current time [19]. There are many different approaches for state estimation depending on the model structure.

We have implemented a very basic and intuitive approach based on the parameter estimation technique of the Grey-Box Buildings toolbox [17]. Instead of estimating the parameters of a model that minimize the measurement residuals, we estimate only the initial states for a model with given parameters. In the present implementation, 24 h of historical measurements are used, and the decision variables of the parameter estimation problem are the initial values of each of the 4 states presented in Fig. 4. The state at the end of the 24 h interval, the current time $t = 0$, is the estimated state. Then, for the measured states $T_{Zon}$ and $T_{Sup}$, instead of using the estimated state, the current measurement is retained.

Finally, in order to obtain a more stable control, the measurement of $T_{Zon}$ is compared to the reference temperature tracking setpoint $T_{Set}$. If $|T_{Zon} - T_{Set}| \leq 0.2$ K, $T_{Zon}$ is taken equal to $T_{Set}$. This correction avoids abrupt changes in the control for small deviations from the set point.

We are aware of the simplicity of the implemented state estimation. It is planned to implement more advanced state estimations in the near future, in particular the approaches described by Vande Cavey et al. and Bonvini et al. [20,21], and analyse their impact on the performance of the MPC.

### 3.5. Optimal control

This subsection details the implementation of the OCP presented by Eq. (1). The control variable $u$ is composed of $\dot{Q}_{GB}$, $\dot{Q}_{HP1}$, $\dot{Q}_{HP2}$ and $\dot{Q}_{Hea}$. Although it is impossible to control the heat consumption of the building $\dot{Q}_{Hea}$ due to the (uncontrolled) manual operation of the heat emission systems, $\dot{Q}_{Hea}$ is required for the model to control thermal comfort in the building. Constraints are put on the positive derivatives of $\dot{Q}_{GB}$, $\dot{Q}_{HP1}$ and $\dot{Q}_{HP2}$ to stabilise the control signals and take into account inertia in the heat production systems. The maximum thermal power of the boiler and electrical power of the heat pumps are limited. Finally, a constraint of 80 °C is put on $T_{Sup}$.

The objective function in Eq. (1) is expanded as a weighted sum of the energy costs $J_c$ and the thermal discomfort cost $J_d$

$$J = J_c + \gamma J_d \tag{3}$$

where $\gamma$ is a weighting variable. The energy costs can be written as

$$J_c = \int_0^{t_h} (c_g \dot{P}_g + c_e \dot{P}_e) \mathrm{d}t \tag{4}$$

with $t_h$ the prediction horizon, $\dot{P}_g$ the gas consumption, $\dot{P}_e$ the electricity consumption, the gas tariff $c_g = 4.3458$ c€/kWh and the electricity tariff $c_e = 7.323$ c€/kWh or 9.431 c€/kWh for low respectively high tariff hours. The high tariff applies every work day between 8 h and 23 h.

**Table 2**
Key performance indicators and normalisation variable for building performance analysis.

| Symb. | Unit | Meaning |
|---|---|---|
| $J_c$ | € | Energy cost |
| $J_e$ | kWh | Primary energy consumption |
| $J_d^*$ | min | Thermal discomfort |
| HDD | K d | Heating degree days (normalisation variable) |

The thermal discomfort cost $J_d$ is implemented as a reference temperature tracking:

$$J_d = \int_0^{t_h} \theta_{occ} (T_{Zon} - T_{Set})^2 \mathrm{d}t \tag{5}$$

where $T_{Zon}$ is the actual zone temperature and $\theta_{occ} = 1$ during occupation and $\theta_{occ} = 0$ elsewhere. The occupation hours are from 07h00 till 19h00 on weekdays. The reference temperature $T_{Set}$ equals 21.8 °C before 24/02/2015 and 21.5 °C after 24/02/2015. This comfort set point is obtained by trial and error on the real building in order to obtain good thermal comfort in each of the zones.

The control time step is 5 min, the open loop control horizon is 1 h. This means that every 5 min, the controller will compute a new control signal by interpolation in the control trajectories of the last solved OCP and transmit these to the building. If the last control trajectories were computed more than 1 h ago, a new state estimation is performed and the OCP will be solved again. The prediction horizon $t_h$ in the OCP is 24 h.

The numerical solution of the OCP is obtained with JModelica.org [22]. Direct collocation is used to discretise time, which reduces the optimisation problem to a nonlinear program (NLP) [23]. JModelica.org utilises third-party NLP solvers, which require first- and second-order derivatives of all expressions in the NLP with respect to all decision variables. CasADi is used to obtain these by algorithmic differentiation [24]. We used the NLP solver IPOPT with the sparse linear solver MA27 from HSL [25,26]. The collocation elements are placed on a regular grid with 15 min interval and two collocation points per element.

## 4. Results

In this section, we compare the performance of the conventional rule-based control (RBC) with the MPC. The comparison is carried out on a daily basis, for working days only. First, the used metrics for the comparison are introduced and then the results are presented.

### 4.1. Metrics for comparison of MPC with RBC

We define three key performance indicators (KPI) and one normalisation variable as shown in Table 2.

The first KPI, the energy cost $J_c$, is computed according to Eq. (4). The second KPI, the primary energy consumption $J_e$, is obtained from

$$J_e = \int_{t_i}^{t_e} (2.5\dot{P}_e + \dot{P}_g) \mathrm{d}t. \tag{6}$$

We use a primary energy factor of 2.5 for electricity and 1.0 for natural gas. The values of $t_i$ and $t_e$ will be given below. As $J_c$ is part of the objective function and $J_e$ is not, it is logic to judge the merits of the MPC on $J_c$. However, in Section 5 we will discuss also the primary energy consumption of both control strategies.

In order to make fair comparisons between days, a time shift is implemented prior to the computation of all metrics. As will be shown later, the MPC will often start the heat pumps long before

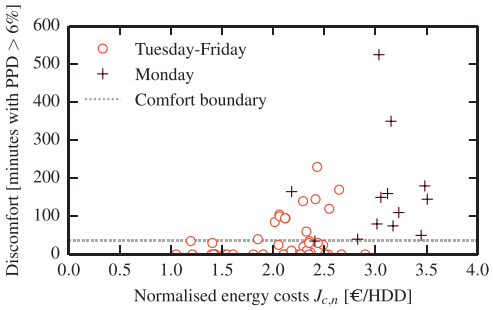


**Fig. 7.** Overview of thermal discomfort and normalised energy costs for all weekdays in the measurement data.

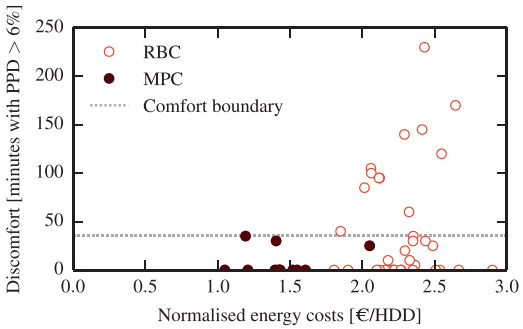


**Fig. 8.** Thermal discomfort and normalised energy costs for Tuesday–Friday, for RBC and MPC.

comfort is required at 07h00 in the morning. Often, one or both heat pumps start at 23h00 in the evening, at the beginning of the low electricity tariff period. Therefore, we shift time so the days start and end at 19h00, the end of the occupation period. As a result, $t_i$ is 19h00 of the previous day, $t_e$ is 19h00 of the analysed day.

Additionally, to cover accidental or intentional heating in the weekend, we add the energy use and costs of the weekend to the KPIs for Monday.

The third KPI, the thermal discomfort $J_d^*$, is not calculated as in Eq. (5). To bring the computation in line with international standards, the thermal discomfort is calculated according to EN 15251 [27]. For every working day, we compute the total time during which thermal comfort is outside the boundaries of category I. This category is defined by a PPD higher than 6%. When taking a clothing factor of 1.0 and a metabolism rate of 1.2, the temperature boundaries corresponding to PPD = 6% are on 21.0 °C and 23.0 °C. As overheating does not occur in the measured data, the practical computation of $J_d^*$ is the total time during working hours where $T_{Zon} \leq 21.0$ °C. We express $J_d^*$ in minutes per day. Next, an acceptable comfort violation is fixed at 5% of the working hours outside of category I. This results in a maximum of 36 min per working day. In other words: when the measured $T_{Zon}$ is less then 36 min below 21.0 °C, the comfort for that day is good.

To normalise the different days, the heating degree days (HDD) are computed on a daily basis, with a base temperature of 16.5 °C. Also for the computation of the HDD the implemented time shift makes sense. The evolution of the ambient temperature during evening and night impacts the heating needs for the future, not the past.

Finally, for some analyses the KPIs are normalised with the HDD for fair comparisons between different days. We denote the normalised KPIs by the subscript $n$.

### 4.2. Comparison of MPC with RBC

Fig. 7 shows the thermal discomfort and normalised energy costs for all weekdays and makes a distinction between Mondays and the other weekdays. The acceptable thermal comfort boundary, 36 min for which PPD > 6%, is also plotted.

The figure shows a large spread in both comfort and costs. On Mondays, the variability is even higher, with on average both a higher discomfort and higher costs than on other weekdays. This is expected because the building is not heated in the weekends. We focus the analysis on Tuesdays–Fridays to increase the similarity between the analysed days.

Fig. 8 is obtained by removing the Mondays and plotting the MPC days in a different colour. Both control strategies are able to provide good thermal comfort on most days, but the RBC has many outliers with bad comfort while the MPC does not have any. It is also clear that the mean normalised costs are lower for MPC than for RBC. This means that on average, the MCP is able to provide a better thermal comfort at a significantly lower cost.

To quantify the savings, only days with acceptable comfort are compared in an energy signature plot [28]. Instead of regressing the primary energy consumption $J_e$ on the heating degree-days, the regression is made on the costs $J_c$ so it is more correct to speak of a cost signature plot. By making a distinction between the RBC and MPC days, the savings can be visualised. This is shown in Fig. 9. The figure shows that despite the use of daily intervals, the regression of daily costs on daily HDD yields a good correlation, in particular for the RBC days. There is more spread on the MPC days, but this is not problematic. Based on both regressions, we have computed the relative daily cost savings: they vary between 30% and 40%. These results are discussed in more detail in the next section.

## 5. Discussion

The MPC is able to provide a similar or better thermal comfort than RBC at a significantly lower energy cost. In this section we try to understand and pinpoint the reasons for the improved performance by analysing the results in more detail.

The mechanism for providing thermal comfort is completely different for both control strategies. The RBC is based on a heating curve with indoor temperature compensation. This means that $T_{Sup}$ is adapted proportionally as a function of $T_{Zon} - T_{Set}$. In the MPC, minimising the deviation from $T_{Set}$ is an explicit objective of the controller. Whenever the building is too cold, the MPC will take abrupt actions to correct $T_{Zon}$. The effectiveness of this correction will depend on the weighting factor $\gamma$ from Eq. (3) and on the general quality of the MPC, which is the result of the cumulative effect of model mismatch, quality of disturbance forecasts and accuracy of the state estimation. When $\gamma$ is sufficiently large and the MPC has no major quality problems, thermal comfort will be guaranteed. The three MPC days with $J_d^*$ close to the boundary of 36 min have

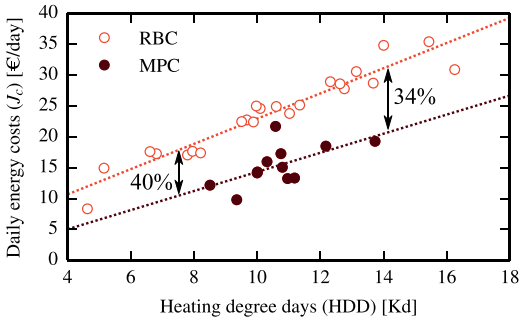


**Fig. 9.** Daily energy costs $J_c$ and savings of MPC versus RBC as a function of heating degree-days (HDD). Only Tuesday–Friday, only days with good thermal comfort.

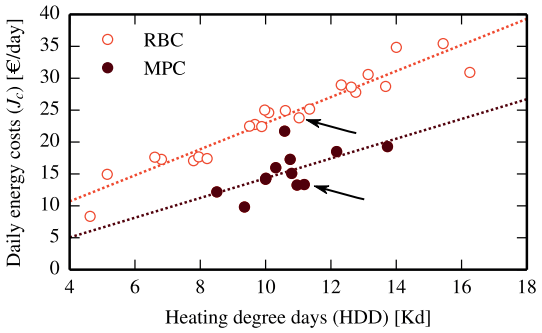


**Fig. 10.** Selection of two similar days for comparing the building operation between RBC and MPC.

suffered from either a large model mismatch, wrong forecasts or a bad state estimation.

The cost savings realised by MPC are large. We analyse the operation of the MPC versus the RBC on two similar days to illustrate typical differences in the control of the heating system. The choice of both days is shown in Fig. 10. A time series plot of the most relevant control and operation variables for these days is shown in Fig. 11. The plot confirms that both days have a similar profile for $T_{Amb}$.

Fig. 11 shows that the control strategy of the MPC is very different from the RBC. A first remarkable difference is the start-up time. The RBC has a weekly schedule, with a start-up at 05h00 in order to reach 21 °C at 07h00 in the morning. The MPC however starts already at midnight and slowly preheats the building. This preheating makes use of the heat pumps at a relatively low supply water temperature $T_{Sup}$. The heat pump power is gradually increased, and so does $T_{Sup}$. Around 06h00, the gas boiler is fired for the purpose of reaching a $T_{Zon}$ of 21.5 °C at 07h00.

A second major difference is the operation of the heat production units. The RBC never uses the heat pumps during this day and this has been confirmed for other days with similar ambient temperatures. The MPC has a model that predicts the performance of each heat production unit. As shown in Eq. (2), these models include the thermal or electrical power, $T_{Amb}$ and $T_{Sup}$. By consequence, the MPC *knows* how to operate these units in such a way that the overall energy costs are minimised. For the studied day, the MPC mainly uses the heat pumps and only operates the gas boiler when the required power $\dot{Q}_{Hea}$ is high.

A third important difference concerns the supply water temperature $T_{Sup}$. The RBC follows the heating curve with room temperature compensation. The supply water reaches a maximum temperature of about 55 °C in the morning and slowly decreases from there for the rest of the day. In contrast, the profile of $T_{Sup}$ in case of MPC is totally different. Interestingly, $T_{Sup}$ is not always lower. We observe three time periods with different behaviour: before 05h00, between 06h00 and 09h00 and after 09h00. In the first period, $T_{Sup}$ rises steadily with increased heat pump power. Around 06h00 the MPC strongly increases the produced power in order to increase $T_{Sup}$ and allow $\dot{Q}_{Hea}$ to rise. In this time block, $T_{Sup}$ reaches even 60 °C. When $T_{Zon}$ has reached $T_{Set}$, the supply water temperature is reduced drastically and stays remarkably low for the rest of the day. The result is a reduction of about 50% of the heat consumption of the building between 09h00 and 19h00. The analysis of different days reveals the same patterns.

Fig. 11 also shows that the MPC does not really meet its target of 21.5 °C at 07h00. This is the consequence of a model mismatch, bad forecasts, a wrong state estimation or a combination of these errors. We can analyse how the MPC expected this specific day to be by comparing the results of the solution of the OCP at 21h00 with the real operation. This is shown in Fig. 12.

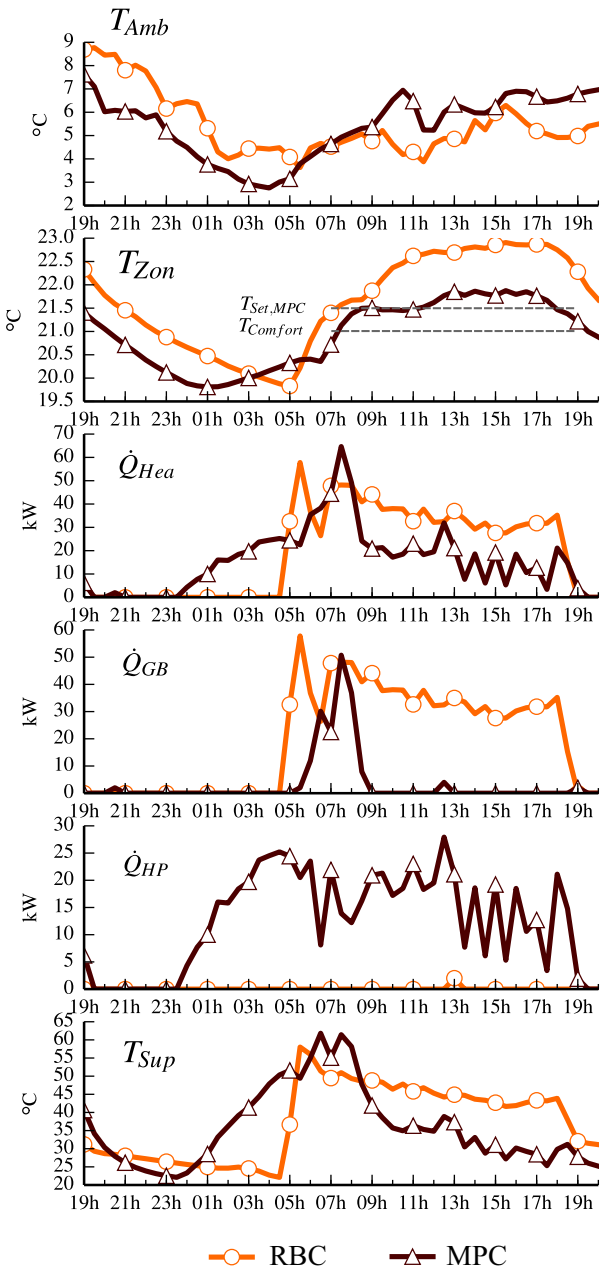


**Fig. 11.** Comparison of operation of two similar days between RBC and MPC. $\dot{Q}_{HP}$ is the sum of $\dot{Q}_{HP1}$ and $\dot{Q}_{HP2}$.

The figure shows a significant difference between the solution of the OCP at 21h00 and the real measured operation of the building with MPC. One of the causes is a wrong forecast of $T_{Amb}$. The locally measured $T_{Amb}$ is higher than the forecasted in the early morning and significantly lower in the afternoon. Nevertheless, this difference cannot explain the missed target of 21.5 °C at 07h00. On the contrary, with the higher ambient temperature it should have been easier to reach the set point.

Before 07h00 there is little or no occupancy and electricity consumption. As ambient temperature, occupancy and plug power are the only forecasted disturbances, this specific error is unlikely to be caused by bad forecasts.

By consequence, the error is a manifestation of errors in the model and/or state estimation. As the real state is not measured and the experiment cannot be repeated, we cannot distinguish between these two sources of error. That is why we are currently developing

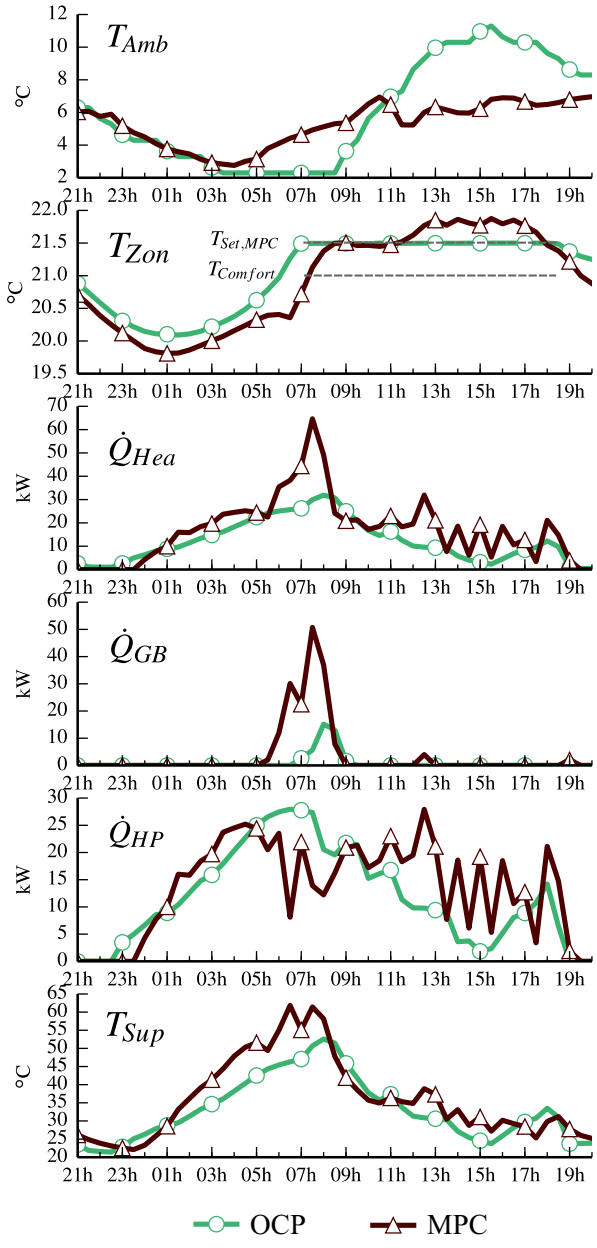


**Fig. 12.** Comparison between expected operation (OCP) and MPC. The OCP was solved at 21h00 with a prediction horizon $t_h$ of 24 h. The MPC has an open-loop horizon of 1 h. $\dot{Q}_{HP}$ is the sum of $\dot{Q}_{HP1}$ and $\dot{Q}_{HP2}$.

a detailed emulator model of the Kalkkaai building on which we can test different versions of MPC under identical boundary conditions. This will be reported in the near future.

Thanks to the feed-back of the building (every hour), the MPC is able to correct the errors. At 06h00 the controller realises that more power is needed in order to reach $T_{Set}$ and starts the gas boiler. One hour later, at the next update, $T_{Set}$ is still not reached. The power of the gas boiler, which was already being reduced by the controller, is increased again. This time this is sufficient to reach the set point around 08h00. The consequence of these actions is a considerably higher $T_{Sup}$ in the morning.

In the afternoon, the MPC adapts to the lower ambient temperature. The heat delivered to the building, $\dot{Q}_{Hea}$ is higher than foreseen by the OCP at 21h00. Nevertheless, the MPC is able to strongly reduce $T_{Sup}$ and operate both heat pumps at a very high efficiency.

**Table 3**
Synthesis of observed differences between RBC and MPC for two similar days.

| Concept | RBC | MPC |
|---|---|---|
| Operating times | Fix schedule | Free. Very early start observed and slow pre-heating of building with low tariff electricity and high COP |
| Hot water supply temperature $T_{Sup}$ | Heating curve with indoor temperature compensation | Free. Mainly lower values of $T_{Sup}$ but also higher values observed. Resulting $T_{Sup}$ depends on dynamic processes |
| Heat production | Mainly condensing gas boiler | Mainly heat pumps at partial load. Gas boiler for peaks |

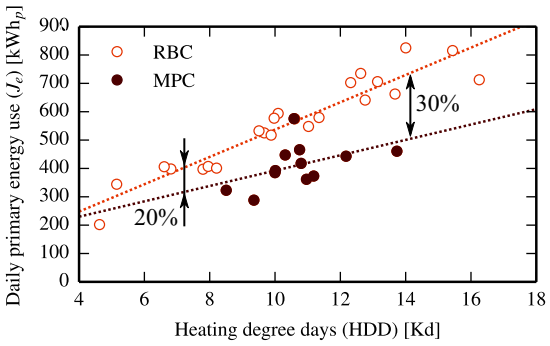


**Fig. 13.** Energy signature showing primary energy use versus heating degree days for both RBC and MPC days. Only Tuesday–Friday, only days with good thermal comfort.

Table 3 summarises the observed differences between the two control strategies on the analysed days. The table distinguishes between three main control concepts: the operation schedule, the supply water temperature and the choice of heat production units.

The objective of the MPC is to minimise energy costs and thermal discomfort. How this translates into primary energy use is visualised in a proper energy signature plot, as shown in Fig. 13. The energy savings are clearly less pronounced than the cost savings but still substantial. In the first place, this is due to the objective in the OCP. A second reason is the electricity tariff. Thanks to low night tariff, the potential for cost savings is larger than for energy savings. Nevertheless, the MPC realises a reduction of primary energy use between 20% and 30% which is a very important added value of the cost driven operational optimisation. This single example may not be generalised, but it illustrates that if the energy tariffs reflect the primary energy content of the different energy vectors to some extent, economical objectives can lead to ecological benefits.

## 6. Conclusion

We have presented the step-by-step implementation of MPC in an office building in Brussels. The control variables are the produced thermal power of the condensing gas boiler and of two identical air/water heat pumps. The MPC makes use of a 4th order grey-box model, simple weekly persistence models for the forecasting of endogenous disturbances and a deterministic state estimation. By introducing rather detailed performance maps for the heat pumps and the boiler, the model knows the implications of the operation on equipment efficiency.

The objective function of the controller is a weighted average of a temperature reference tracking and energy costs. The MPC has been operated in real-time in the winter of 2014–2015 and is compared to the conventional RBC control.

The results show an average cost saving between 34% and 40% compared to the reference control. Even the primary energy use,

which is not directly covered by the objective function, is decreased by more than 20%.

The main differences between the MPC and RBC strategies are that the MPC uses the heat pumps much more, starts up very early to pre-heat the building and strongly reduces the supply water temperature once the comfort set point has been reached.

On the one hand, the energy savings would have been smaller if the conventional control had used the heat pumps more often. On the other hand, these savings are realised with an MPC containing many simplifications in different steps of the process. There is still room for improving the MPC performance. The results of this single experiment cannot be generalised but they are certainly encouraging towards the use of MPC for controlling thermal systems in buildings.

## Acknowledgements

The authors gratefully acknowledge the following projects and institutes for supporting this work:

- the FP7 project *PerformancePlus* funded by the European Commission (KU Leuven, contract nb. 308991),
- the project *Optimal energy networks for buildings* funded by the KU Leuven Energy Institute (KU Leuven),
- *Flexipac* funded by the Région Wallonne, DGO4 (3E, contract nb. 1250570).

## References

[1] M. Ardehali, T.F. Smith, Literature Review to Identify Existing Case Studies of Controls-related Energy-inefficiency in Buildings for National Building Controls Information Program, Tech. Rep., University of Iowa, Department of Mechanical Engineering, Iowa City, Iowa, 2001.
[2] D. Gyalistras, M. Gwerder, F. Oldewurtel, C.N. Jones, M. Morari, B. Lehmann, K. Wirth, V. Stauch, Analysis of energy savings potentials for integrated room automation, in: 10th RHEVA World Congress CLIMA, REHVA, Antalya, Turkey, 2010.
[3] G. Henze, D. Kalz, S. Liu, C. Felsmann, Experimental analysis of model-based predictive optimal control for active and passive building thermal storage inventory, HVAC&R Res. 11 (2) (2005) 189–213, http://dx.doi.org/10.1080/10789669.2005.10391134.
[4] S. Prívara, J. Široký, L. Ferkl, J. Cigler, Model predictive control of a building heating system: the first experience, Energy Build. 43 (2–3) (2011) 564–572, http://dx.doi.org/10.1016/j.enbuild.2010.10.022.
[5] F. Oldewurtel, A. Parisio, C.N. Jones, D. Gyalistras, M. Gwerder, V. Stauch, B. Lehmann, M. Morari, Use of model predictive control and weather forecasts for energy efficient building climate control, Energy Build. 45 (2011) 15–27, http://dx.doi.org/10.1016/j.enbuild.2011.09.022.
[6] C. Verhelst, F. Logist, J. Van Impe, L. Helsen, Study of the optimal control problem formulation for modulating air-to-water heat pumps connected to a residential floor heating system, Energy Build. 45 (2011) 43–53, http://dx.doi.org/10.1016/j.enbuild.2011.10.015.
[7] M. Gruber, A. Trüschel, J.-O. Dalenbäck, Model-based controllers for indoor climate control in office buildings – complexity and performance evaluation, Energy Build. 68 (2014) 213–222, http://dx.doi.org/10.1016/j.enbuild.2013.09.019.
[8] M. Gwerder, D. Gyalistras, C. Sagerschnig, R.S. Smith, D. Sturzenegger, Final Report: Use of Weather And Occupancy Forecasts for Optimal Building Climate Control. Part II: Demonstration (OptiControl-II), Tech. Rep., Automatic Control Laboratory, ETH, Zurich, Switzerland, September 2013.
[9] P. Li, D. Li, D. Vrabie, S. Bengea, S. Mijanovic, Experimental demonstration of model predictive control in a medium-sized commercial building, in: 3rd International High Performance Buildings Conference, Purdue, 2014.
[10] S.C. Bengea, A.D. Kelman, F. Borrelli, R. Taylor, S. Narayanan, Implementation of model predictive control for an HVAC system in a mid-size commercial building, HVAC&R Res. 20 (2014) 121–135, http://dx.doi.org/10.1080/10789669.2013.834781.
[11] G.S. Pavlak, G.P. Henze, V.J. Cushing, Optimizing commercial building participation in energy and ancillary service markets, Energy Build. 81 (2014) 115–126, http://dx.doi.org/10.1016/j.enbuild.2014.05.048.
[12] J.E. Braun, Reducing energy costs and peak electrical demand through optimal control of building thermal storage, ASHRAE Trans. 96 (2) (1990) 876–888.
[13] C. Verhelst, Model Predictive Control of Ground Coupled Heat Pump Systems for Office Buildings (Ph.D. thesis), KU Leuven, 2012.
[14] E. Lorenz, J. Hurka, D. Heinemann, H.G. Beyer, Irradiance forecasting for the power prediction of grid-connected photovoltaic systems, IEEE J. Select. Top. Appl. Earth Obs. Remote Sens. 2 (1) (2009) 2–10, http://dx.doi.org/10.1109/JSTARS.2009.2020300.
[15] E. Lorenz, J. Kühnert, D. Heinemann, Short term forecasting of solar irradiance by combining satellite data and numerical weather predictions, in: 27th European Photovoltaic Solar Energy Conference and Exhibition, 2012, pp. 4401–4405.
[16] P. Undén, L. Rontu, H. Järvinen, P. Lynch, J. Calvo, HIRLAM-5 Scientific Documentation, Tech. Rep., SMHI, Norrköping, Sweden, 2002.
[17] R. De Coninck, F. Magnusson, J. Åkesson, L. Helsen, Toolbox for development and validation of grey-box building models for forecasting and control, J. Build. Perform. Simul. (2015), http://dx.doi.org/10.1080/19401493.2015.1046933.
[18] S. Seabold, J. Perktold, Statsmodels: econometric and statistical modeling with python, in: Proceedings of the 9th Python in Science Conference (Scipy 2010), 2010, pp. 57–61.
[19] J. Rawlings, D. Mayne, Model Predictive Control – Theory and Design, 2013, http://dx.doi.org/10.1002/9781119941446.ch3.
[20] M. Vande Cavey, R. De Coninck, L. Helsen, Setting up a framework for model predictive control with moving horizon state estimation using JModelica, in: 10th International Modelica Conference, Lund, Sweden, 2014, pp. 1295–1303, http://dx.doi.org/10.3384/ECP140961295.
[21] M. Bonvini, M.D. Sohn, J. Granderson, M. Wetter, M.A. Piette, Robust on-line fault detection diagnosis for HVAC components based on nonlinear state estimation techniques, Appl. Energy 124 (2014) 156–166, http://dx.doi.org/10.1016/j.apenergy.2014.03.009.
[22] J. Åkesson, K.-E. Årzén, M. Gäfvert, T. Bergdahl, H. Tummescheit, Modeling and optimization with Optimica and JModelica.org – languages and tools for solving large-scale dynamic optimization problems, Comput. Chem. Eng. 34 (11) (2010) 1737–1749, http://dx.doi.org/10.1016/j.compchemeng.2009.11.011.
[23] F. Magnusson, J. Åkesson, Collocation methods for optimization in a Modelica environment, in: 9th International Modelica Conference, Munich, Germany, 2012.
[24] J. Andersson, J. Åkesson, M. Diehl, CasADi – A symbolic package for automatic differentiation and optimal control, in: S. Forth, P. Hovland, E. Phipps, J. Utke, A. Walther (Eds.), Recent Advances in Algorithmic Differentiation, Lecture Notes in Computational Science and Engineering, Springer, Berlin, 2012.
[25] A. Wächter, L.T. Biegler, On the implementation of a primal-dual interior point filter line search algorithm for large-scale nonlinear programming, Math. Program. 106 (1) (2006) 25–57.
[26] HSL, A collection of Fortran codes for large scale scientific computation. http://www.hsl.rl.ac.uk (accessed 14.1.15).
[27] CEN, EN 15251:2007. Indoor Environmental Input Parameters for Design and Assessment of Energy Performance of Buildings Addressing Indoor Air Quality, Thermal Environment, Lighting and Acoustics, 2007.
[28] A. Rabl, A. Rialhe, Energy signature models for commercial buildings: test with measured data and interpretation, Energy Build. 19 (1992) 143–154.